Increased renal adrenomedullin expression in rats with ureteral obstruction

Rikke Nørregaard,[1,2]***** **Tina Bødker,**[1,2]***** **Boye L. Jensen,**[4] **Lene Stødkilde,**[1,2] **Søren Nielsen,**[1,3] **and Jørgen Frøkiær**[1,2]

[1]*The Water and Salt Research Center,* [2]*Institute of Clinical Medicine,* and [3]*Institute of Anatomy, University of Aarhus, Aarhus, Denmark; and* [4]*Department of Physiology and Pharmacology, University of Southern Denmark, Odense, Denmark*

Nørregaard R, Bødker T, Jensen BL, Stødkilde L, Nielsen S, Frøkiær J. Increased renal adrenomedullin expression in rats with ureteral obstruction. *Am J Physiol Regul Integr Comp Physiol* 296: R185–R192, 2009. First published October 22, 2008; doi:10.1152/ajpregu.00170.2008.—Ureteral obstruction is characterized by decreased renal blood flow that is associated with hypoxia within the kidney. Adrenomedullin (AM) is a peptide hormone with tissue-protective capacity that is stimulated through hypoxia. We tested the hypothesis that ureteral obstruction stimulates expression of AM and hypoxia-inducible factor-1 (HIF-1α) in kidneys. Rats were exposed to bilateral ureteral obstruction (BUO) for 2, 6, 12, and 24 h or sham operation and compared with unilateral obstruction (UUO). AM mRNA expression was measured by quantitative PCR in cortex and outer medulla (C+OM) and inner medulla (IM). AM and HIF-1α protein abundance and localization were determined in rats subjected to 24-h BUO. AM mRNA expression in C+OM increased significantly after 12-h BUO and further increased after 24 h. In IM, AM mRNA expression increased significantly in response to BUO for 6 h and further increased after 24 h. AM peptide abundance was enhanced in C+OM and IM after 24-h BUO. Immunohistochemical labeling of kidneys showed a wider distribution and more intense AM signal in 24-h BUO compared with Sham. In UUO rats, AM mRNA expression increased significantly in IM of the obstructed kidney compared with nonobstructed and Sham kidney whereas AM peptide increased in IM compared with Sham. HIF-1α protein abundance increased significantly in IM after 24-h BUO compared with Sham and HIF-1α immunoreactive protein colocalized with AM. In summary, AM and HIF-1α expression increases in response to ureteral obstruction in agreement with expected oxygen gradients. Hypoxia acting through HIF-1α accumulation may be an important pathway for the renal response to ureteral obstruction.

hypoxia-inducible factor-1α; bilateral ureteral obstruction; medullary hypoxia; inflammation; tumor neurosis factor α

THE VASODILATOR PEPTIDE ADRENOMEDULLIN (AM) was discovered in human pheochromocytoma cell extracts by its ability to initiate cAMP production in target cells (26). AM is expressed in most tissues and released to plasma at a rate that reflects transcription (22, 42, 48). AM acts primarily in a paracrine fashion and its effects are mediated through binding to a specific receptor that comprises a complex between receptor activity-modifying proteins (RAMPs) and calcitonin receptor-like receptor (CRLR) (23, 24). AM increases total renal blood flow and regional flow to cortex and medulla (12, 17, 22, 28, 42, 46, 48). AM induces natriuresis and diuresis by increasing glomerular filtration rate and fractional sodium excretion and reducing distal tubular sodium reabsorption (21, 22). AM is stimulated in a variety of pathophysiological conditions characterized by hypoxia, such as cardiovascular, respiratory, and renal disorders (2, 4, 43, 45). The hypoxia-induced transcription of the AM gene is dependent on the hypoxia-inducible factor-1α (HIF-1α) transcription factor (38). Under hypoxic conditions HIF-1α dimerizes with HIF-1β, the other subunit of HIF-1 (that is not regulated by O_2 levels), and this heterodimer HIF-1 translocates to the nucleus where the activation of target genes is mediated by binding to hypoxia-response elements (6, 20, 29, 45). HIF-1α displays a hypoxia-dependent distribution within the kidney (6, 26, 40, 51). Importantly, in patients with ureteropelvic junction obstruction HIF is stimulated in the smooth muscles of the urinary tract and in urothelial cells (41). Moreover, it has been demonstrated that HIF-1α is upregulated in the bladder in response to partially bladder outlet obstruction (9). On the basis of these observations it appears that ureteral obstruction is associated with stimulation of HIF-1α in different segments of the urinary tract, but there is currently no data available on the regulation of HIF-1α and downstream HIF gene targets such as AM in the kidney in response to ureteral obstruction. Ureteral obstruction leads to an immediate preglomerular, transient vasodilatation followed by a long-lasting vasoconstriction simultaneous with an increase in the ureteral pressure (35, 50, 53). In response to 24 h of bilateral ureteral obstruction (BUO; 24-h BUO), there is a decrease in the outer cortical perfusion of ~20% (16, 47), whereas the total renal blood flow (RBF) is decreased to 40–70% of control values in the kidney (15, 34). This leads to decreased O_2 delivery and potentially to subsequent hypoxia in the kidney tissue (54). If obstruction persists, this in turn leads to interstitial inflammation, fibrosis, tubular atrophy, and renal failure (1, 47). As shown for renal vascular disorders (44), AM could also be involved in a hypoxia-induced protective response in the obstructed kidney governed by accumulation of HIF-1α. We therefore hypothesized that AM mRNA and protein levels would increase in the kidney in response to ureteral obstruction in keeping with expected oxygen gradients and depending on activation of HIF-1α. To address the hypothesis, a kinetic study was performed, and the temporal and spatial correlation between changes in renal tissue AM and HIF-1α expression was determined in renal tissue subjected to bilateral and unilateral ureteral ligation.

MATERIALS AND METHODS

In vivo rat experiments. All animal experiments were conducted in accordance with the Danish legislation for the care and handling of animals and also with the guidelines published by the National

***** R. Nørregaard and *T. Bødker contributed equally to this study.

Address for reprint requests and other correspondence: J. Frøkiær, The Water and Salt Research Center, Clinical Institute, Univ. of Aarhus, Dept. of Clinical Physiology and Nuclear Medicine, Aarhus Univ. Hospital-Skejby, Brendstrupgaardsvej, DK-8200 Aarhus N, Denmark (e-mail: jf@ki.au.dk).
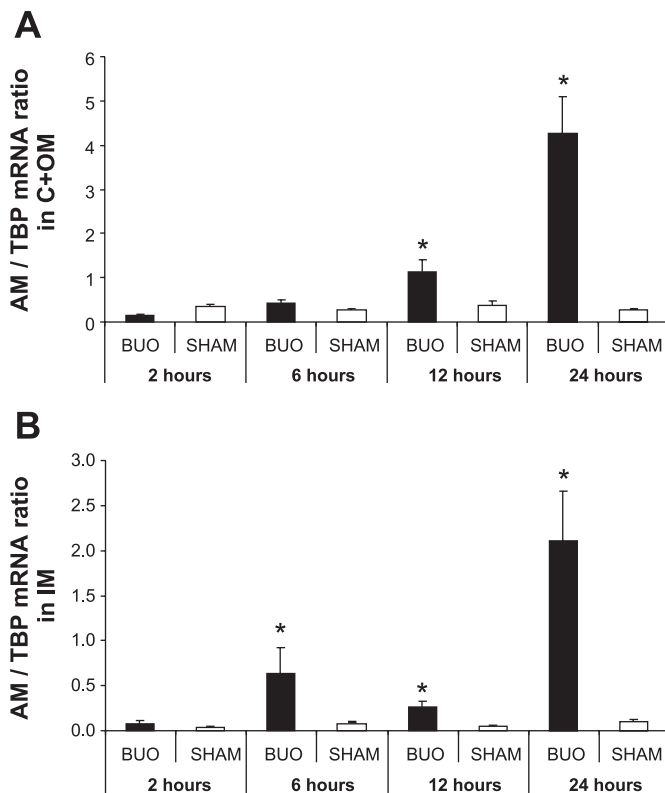
A

B

Fig. 1. Expression of adrenomedullin (AM) mRNA in cortex + outer medulla (C+OM) and inner medulla (IM) from sham-operated (Sham) rats and rats subjected to 2-, 6-, 12-, and 24-h bilateral ureteral obstruction (BUO). Representative quantitative PCR (QPCR) for AM/TATA box binding protein (TBP) mRNA level. QPCR was performed using 100 ng cDNA. Analysis of all the samples from sham-operated ($n = 6$) and obstructed kidneys of rats with BUO ($n = 6$) revealed that there was an increase of AM mRNA level in C+OM after 12- and 24-h BUO compared with sham-operated rats (A). In IM, AM mRNA level was increased after 6-, 12-, and 24-h BUO compared with sham-operated rats (B). Bars represent means ± SE. *$P < 0.05$ BUO compared with Sham rats.

Institutes of Health. Furthermore, the animal protocols were approved by the board of the Institute of Clinical Medicine, University of Aarhus, according to the licenses for use of experimental animals issued by the Danish Ministry of Justice.

Male Munich-Wistar rats (Møllegaard Breeding Centre, Eiby, Denmark) initially weighing 220 g were used. They had free access to tap water and standard feed (Altromin, Lage, Germany). During the experiments, rats were kept with a 12:12-h light-dark cycle, a temperature of $21 \pm 2°C$, and humidity of 55%. Rats were anesthetized with a mixture of O_2, N_2O, and isoflurane in the ratio 4:3:2 and placed on a heating pad to maintain rectal temperature at 37–38°C. The abdomen was opened with a midline incision, and two ureters were exposed and ligated with a 5-0 silk ligature to perform the obstruction. The abdomen was closed with 2-0 prolene suture and the skin was closed with 2-0 polysorb. Finally, rats were given 0.1 ml of TemGesic (0.3 mg/ml, Schering-Plough, Farum, Denmark) for analgesia and regained consciousness afterward.

All rats were allocated to the protocols below. Weight-matched sham-operated animals (Sham) were observed and prepared in parallel with each group as follows.

Protocol 1: *1*) BUO was induced for 2 h. Kidneys were prepared for quantitative PCR ($n = 6$). *2*) Sham-operated controls were prepared in parallel ($n = 6$).

Protocol 2: *1*) BUO was induced for 6 h. Kidneys were prepared for quantitative PCR ($n = 6$). *2*) Sham-operated controls were prepared in parallel ($n = 6$).

Protocol 3: *1*) BUO was induced for 12 h. Kidneys were prepared for quantitative PCR ($n = 6$). *2*) Sham-operated controls were prepared in parallel ($n = 6$).

Protocol 4: BUO was induced for 24 h ($n = 18$) and the kidneys were removed and prepared for quantitative PCR, protein isolation ($n = 14$), and immunohistochemistry (IHC) ($n = 4$). For matched sham-operated control rats ($n = 16$), kidneys were prepared for quantitative PCR, protein isolation ($n = 12$), and IHC ($n = 4$).

Protocol 5: *1*) Unilateral ureteral obstruction (UUO) was induced for 24 h ($n = 16$). Kidneys were prepared for quantitative PCR ($n = 6$), protein isolation ($n = 6$), and IHC ($n = 4$) for AM. *2*) Sham-operated controls rats ($n = 16$) were prepared in parallel for quantitative PCR ($n = 6$), protein isolation ($n = 6$), and IHC ($n = 4$).

RNA extraction and cDNA synthesis. RNA extraction was performed according to the protocol of Qiagen's RNeasy mini kit. Approximately 30 mg of kidney tissue was used for isolation, and the RNA concentration was quantified by measuring the optical density at 260 nM on BioPhotometer 6131, Eppendorf, Hamburg, Germany. cDNA synthesis was performed with StrataScript First-Strand synthesis system (Stratagene, AH Diagnostics, Aarhus, Denmark) in accordance to the manufacturer's instructions.

Quantitative PCR. For quantitative PCR, 100 ng cDNA served as a template for PCR amplification using Brilliant SYBR Green QPCR Master Mix, according to the manufacturer's instructions, (Stratagene, AH Diagnostics, Aarhus, Denmark). Serial dilution (1 ng to 1 fg/μl) of cDNA was used as a template for generation of a standard curve. Standards and unknown samples were amplified in duplicate in 96-well plates, and PCR was performed for 40 cycles consisting of denaturation for 30 s at 95°C followed by annealing and polymerization at 60°C for 45 s. Emitted fluorescence was detected during the annealing/extension step in each cycle. Specificity was ensured by postrun melting curve analysis. 18S and TATA box binding protein were used as housekeeping genes for standardization. In this study we used the following primer sequences: rat AM, sense 5′-GCA GTT CCG AAA GAA GTG GAA-3′; rat AM, antisense 5′-GCT GCT GGA CGC TTG TAG TTC-3′ (GenBank acc. no. NM_012715); rat 18S, sense 5′-CAT GGC CGT TCT TAG TTG-3′; rat 18S antisense 5′-CAT GCC AGA GTC TCG TTC-3′ (GenBank acc. no. M11188); TATA box binding protein, sense GAC TCC TGT CTC CCC TAC CC, antisense CTC AGT GCA GAG GAG GGA AC (GenBank acc. no. NM_001004198).

AM measurements in tissue after 24-h BUO and 24-h UUO. Protein was isolated by homogenization of tissue in lysis buffer (1 mM Tris·HCl, 10 mM EDTA, and 1 mM DTT) with protease inhibitor mix (Mini complete Protease Inhibitor; Roche Diagnostics, Vedbaek, Denmark at pH 7.2). Subsequently, 10 μl of Triton X-100 [10% (wt/vol) final concentration] was added followed by centrifugation at 11,000 g at 4°C for 10 min. The supernatant was removed and
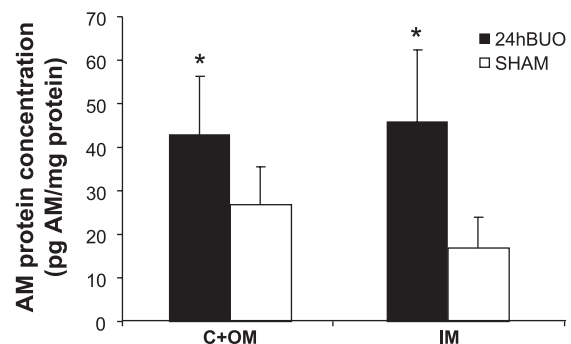

Fig. 2. AM protein concentration in C+OM and IM from 24-h BUO ($n = 6$) and Sham control ($n = 6$) rats was measured by ELISA. AM concentration increases significantly in C+OM and IM in response to 24-h BUO. Bars represent means ± SE. *$P < 0.05$ BUO compared with Sham rats.

centrifuged again at 11,000 g at 4°C for 10 min. Protein concentration was measured by Pierce BCA protein assay kit (Roche Diagnostics). The AM protein concentration was measured in the homogenate with a commercial enzyme immunoassay kit (Phoenix Pharmaceuticals).

Preparation of nuclear extraction. For HIF-1α Western analysis, nuclear proteins, both snap-frozen cortex and IM, were extracted by using the Nuclear Extraction Kit according to manufacturer's protocol (no. FNN0031; Biosource, San Jose, CA). Protein concentration was measured by Pierce BCA protein assay kit (Roche Diagnostics).

Western blot analysis. Samples of nuclear fraction from the cortex and IM were run on a 12% polyacrylamide minigel (Bio-Rad Mini Protean II). For each gel, an identical gel was run in parallel and subjected to Coomassie staining. The Coomassie-stained gel was applied to determine identical loading or to allow for correction for minor variations in loading.

Protein (50 μg) was loaded on 12% polyacrylamide minigels. Proteins were transferred to a nitrocellulose membrane (Hybond ECL RPN 3032D, Amersham Pharmacia Biotech, Amersham, UK). Afterward the blots were blocked with 5% nonfat dry milk in PBS-T (80 mM Na_2HPO_4, 20 mM NaH_2PO_4, 100 mM NaCl, 0.1 Tween 20, adjusted to pH 7.4). After being washed with PBS-T the blots were incubated with HIF-1α antibody overnight at 4°C. Antigen-antibody complex was visualized with horseradish peroxidase-conjugated secondary antibodies (P447, diluted 1:3,000, Dako, Glostrup, Denmark) using enhanced chemiluminescence system (ECL, Amersham Pharmacia Biotech).

Primary antibody. AM: rabbit anti-AM 1-50 (rat) serum (Phoenix Pharmaceuticals, cat. no. H-010-08). HIF-1α: mouse anti-HIF-1α (Novus Biologicals, cat. no. NB 100-105).

IHC. Kidneys from the sham-operated control rats and obstructed rats were fixated by retrograde perfusion via the abdominal aorta with 3% paraformaldehyde in 0.1 M PBS buffer, pH 7.4. Afterward the kidneys were immersion fixed for 1 h and washed 3 × 10 min with 0.1 M PBS buffer. The kidney blocks were dehydrated and embedded in paraffin. The paraffin-embedded tissues were cut in 2-μm sections on a rotary microtome (Leica Microsystems, Herlev, Denmark). For immunoperoxidase labeling, the sections were deparaffinized and

rehydrated. Endogenous peroxidase activity was blocked with 5% H_2O_2 in absolute methanol for 10 min at room temperature. Kidney sections were boiled in a target retrieval solution (1 mmol/l Tris, pH 9.0, with 0.5 mM EGTA) for 10 min to expose antigens. After cooling, nonspecific binding was prevented by incubating the sections in 50 mM NH_4Cl in PBS for 30 min followed by blocking in PBS containing 1% BSA, 0.05% saponin, and 0.2% gelatin. Sections were incubated with primary antibody diluted in PBS with 0.1% BSA and 0.3% Triton X-100 overnight at 4°C. After being washed 3 × 10 min with PBS (supplemented with 0.1% BSA, 0.05% saponin, and 0.2% gelatin), the sections were incubated with horseradish peroxidase-conjugated secondary antibody (P448, goat anti-rabbit immunoglobulin, DAKO, Glostrup, Denmark) for 1 h at room temperature. After being rinsed with PBS wash buffer, the sites of antibody-antigen reactions were visualized with 0.05% 3,3′-diaminobenzidine tetrachloride (Kem-en Tek, Copenhagen, Denmark) dissolved in distilled water with 0.1% H_2O_2. Light microscopy was carried out with a Leica DMRE (Leica Microsystem).

TNF-α measurements in IM after 24-h BUO. Protein was isolated by homogenization of tissue in homogenization buffer (10 mM HEPES, pH 7.9, 10 mM KCl, 0.1 mM EGTA, 1 mM DTT, and 0.5 mM PMSF). The homogenate was centrifuged at 3,000 g at 4°C for 15 min. The supernatant was removed and the protein concentration was measured by Pierce BCA protein assay kit (Roche Diagnostics). The TNF-α protein concentration was measured in the homogenate using a commercial enzyme immunometric assay kit (Assay Designs, Ann Arbor, MI).

Statistics. Values are presented as means ± SE. Statistical comparisons between experimental groups were made by a standard unpaired *t*-test. P values < 0.05 were considered significant.

RESULTS

Effect of BUO on renal AM expression and localization. C+OM and IM tissue fraction was harvested at 2, 6, 12, and 24 h after BUO and analyzed for AM mRNA and peptide level. The expression of AM mRNA first increased significantly in
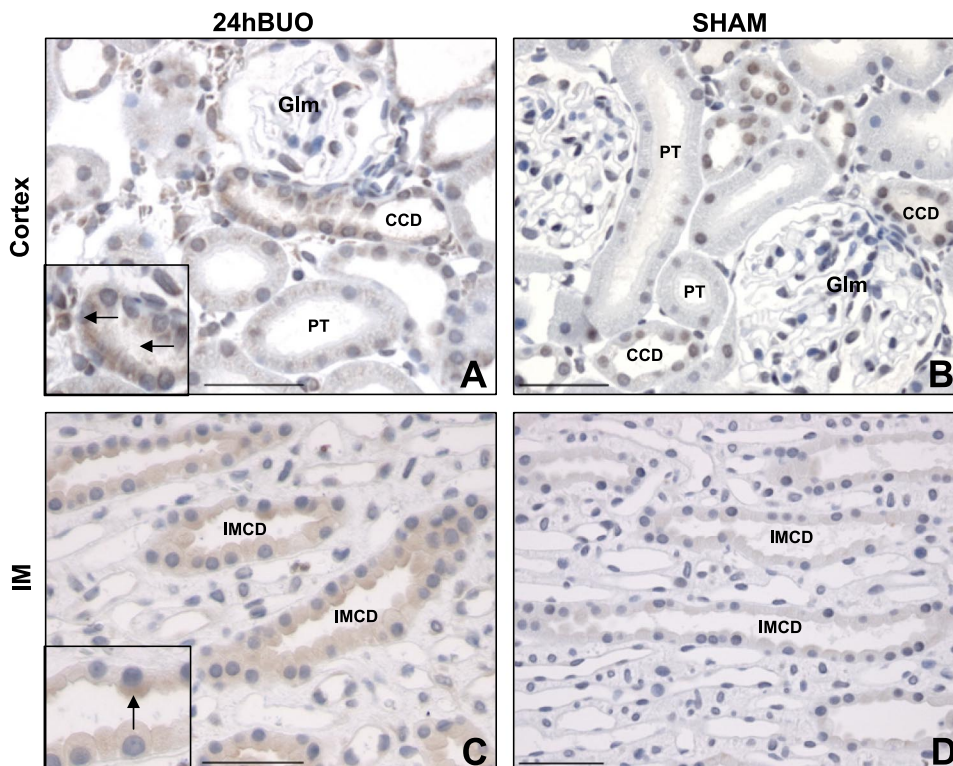

Fig. 3. Immunohistochemistry for AM in kidney cortex and IM of 24-h BUO (*A* and *C*) and sham-operated rats (*B* and *D*). *A*: in cortex from obstructed kidneys, immunolabeling for AM was associated with proximal tubuli (PT), connecting tubuli, glomeruli (Glm), interstitial cells, and cortical collecting ducts (CCD). *B*: in cortex from control kidneys, AM immunoreactivity was associated with connecting tubuli and cortical collecting ducts. *C*: in IM from obstructed kidneys, significant immunoreactivity for AM was associated with inner medullary collecting ducts (IMCD), thin limbs of Henle's loop, papillary epithelium, and interstitial cells. Arrows (*A* and *C*) indicate marked labeling in collecting duct in both cortex and IM. *D*: in IM from control kidneys, AM immunoreactivity was associated with IMCD and thin limbs of Henle's loop. Bar = 50 μm.

C+OM 12 h after BUO and further increased at 24 h of BUO compared with Sham (Fig. 1A). In IM, the AM mRNA level was first increased significantly after 6- and 12-h BUO compared with Sham and further augmented after 24-h BUO (Fig. 1B). There was a significant higher AM peptide tissue concentration in IM from 24-h BUO rats (45.8 ± 16.6 pg/mg of protein) compared with sham-operated control rats (16.8 ± 7.3 pg/mg of protein). Also in cortex, the AM concentration was increased in response to 24-h BUO (43 ± 13.1 vs. 27 ± 8.5 pg/mg of protein) (Fig. 2).

To address cellular localization of AM, we applied a rabbit anti-rat AM antibody to sections of perfusion-fixed kidneys from sham-operated control rats and from rats subjected to 24-h BUO. Immunohistochemical analysis showed more intense labeling of cortex and IM for AM protein in the 24-h BUO rats (Fig. 3, A and C) compared with Sham (Fig. 3, B and D). There was no obvious difference in the staining intensity between obstruction and nonobstructed kidneys in outer medulla (not shown). In kidneys from sham-operated control rats, AM signals were associated with the connecting tubules and collecting ducts in cortex (Fig. 3B). In the obstructed kidney, AM immunoreactivity was more widespread and associated with the proximal tubules, glomerulus, interstitial cells, and collecting ducts (Fig. 3A). In the outer medulla, AM immunoreactivity was associated with collecting ducts and the thick ascending limb of Henle's loop. In the IM of kidneys from sham-operated control rats, AM was localized in the thin limbs of Henle's loop and collecting ducts (Fig. 3D). In kidneys from BUO rats there was labeling of collecting ducts, thin limbs of the loop of Henle, and interstitial cells (Fig. 3C).

Effect of UUO on renal AM expression and localization. Next, the effect of 24-h UUO on AM expression was examined. In the C+OM tissue fraction, AM mRNA level was elevated compared with Sham in both the obstructed and nonobstructed kidneys, and there was no difference between AM mRNA level in obstructed and nonobstructed kidneys in rats with UUO (Fig. 4A). AM mRNA level in IM was markedly increased in the obstructed kidney compared with both the nonobstructed kidneys and sham-operated rats (Fig. 4A). There was no difference in AM mRNA expression between nonobstructed and Sham kidney (Fig. 4A). AM peptide tissue concentration in C+OM was not significantly different between the three groups (Fig. 4B). AM peptide concentration in IM was significantly higher in the obstructed kidney compared with Sham. There was no difference in AM concentration between nonobstructed and obstructed kidney (Fig. 4B).

IHC showed that AM immunoreactivity was associated with IM collecting ducts, thin limbs of Henle's loop, and interstitial cells in obstructed kidney IM compared with faint labeling of similar renal segments in contralateral kidneys and sham-operated control rats (Fig. 5). There was no change in labeling intensity in renal cortex between the obstructed and nonobstructed kidneys. In general, AM protein immunoreactivity was stronger in the obstructed and nonobstructed kidneys compared with kidneys from sham-operated control rats, and the labeling was associated with the same segments as kidneys from BUO rats (data not shown).

Effect of BUO for 24 h on renal HIF-1α expression and localization. Semiquantitative immunoblotting experiments of nuclear extract from both BUO and sham-operated control rats for HIF-1α revealed an elevated abundance of HIF-1α protein
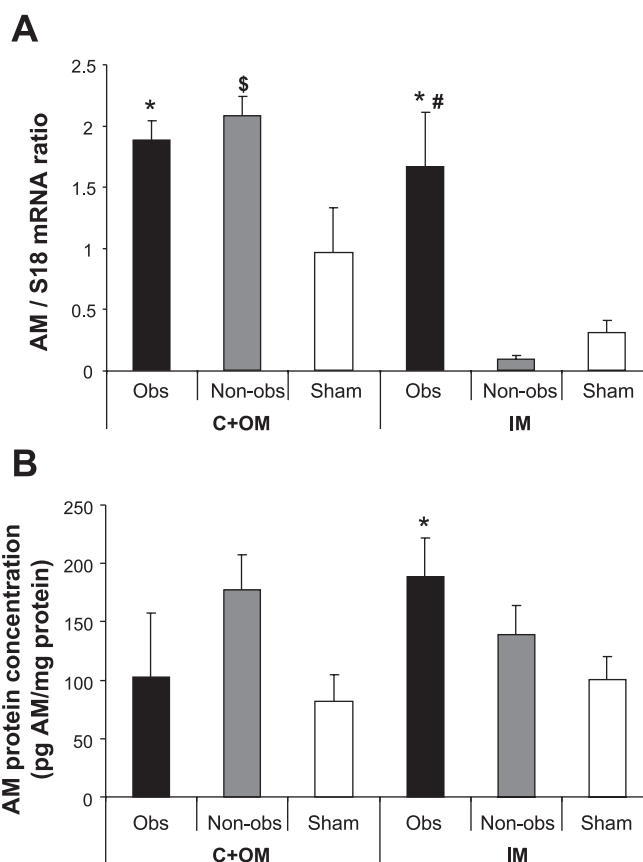
Fig. 4. Expression of AM mRNA and concentration of AM protein in C+OM and IM from Sham rats ($n = 6$) and rats subjected to 24-h unilateral ureteral obstruction (UUO) ($n = 6$). A: representative QPCR for AM/18S mRNA level. QPCR was performed using 100 ng cDNA. Analysis of all the samples from Sham and obstructed (Obs) kidneys of rats with 24-h UUO revealed that there was an increase of AM mRNA level in the obstructed and contralateral kidney compared with Sham rats in C+OM. In IM, AM mRNA level was only increased in the obstructed kidney compared with both the nonobstructed (Non-obs) kidney and kidneys from Sham rats. Bars represent means $\pm$ SE. *$P < 0.05$ obstructed kidney from 24-h UUO compared with Sham rats. $$P < 0.05$ nonobstructed kidney from 24-h UUO compared with Sham rats. #$P < 0.05$ obstructed kidney compared with nonobstructed kidney from 24-h UUO rats. B: AM concentration was not changed between the 3 groups in C+OM. However, in IM the AM concentration was increased significantly in the obstructed kidney from 24-h UUO compared with Sham rats. Bars represent means $\pm$ SE. *$P < 0.05$ obstructed kidney from 24-h UUO compared with Sham rats.

in IM in response to 24-h BUO compared with Sham. There was no difference in HIF-1α expression between the two groups in cortex (Fig. 6A). Immunohistochemical labeling of kidney sections for HIF-1α showed that immunoreactive HIF-1α protein was associated with cell nuclei and cytoplasma in the medullary collecting ducts, interstitial cells, and thin limbs of the loop of Henle, and there was a marked increase in the HIF-1α labeling in the obstructed kidneys (Fig. 6B) compared with sham-operated control rats (Fig. 6C).

To test whether HIF-1α and AM localize in the same kidney segments in the papillary tip in response to 24-h BUO, consecutive tissue sections were stained for HIF-1α and AM. IHC demonstrated that HIF-1α and AM in two pairs of consecutive sections was localized in the same kidney segments, namely medullary colleting ducts, interstitial cells, and thin limbs of the loop of Henle (Fig. 7).
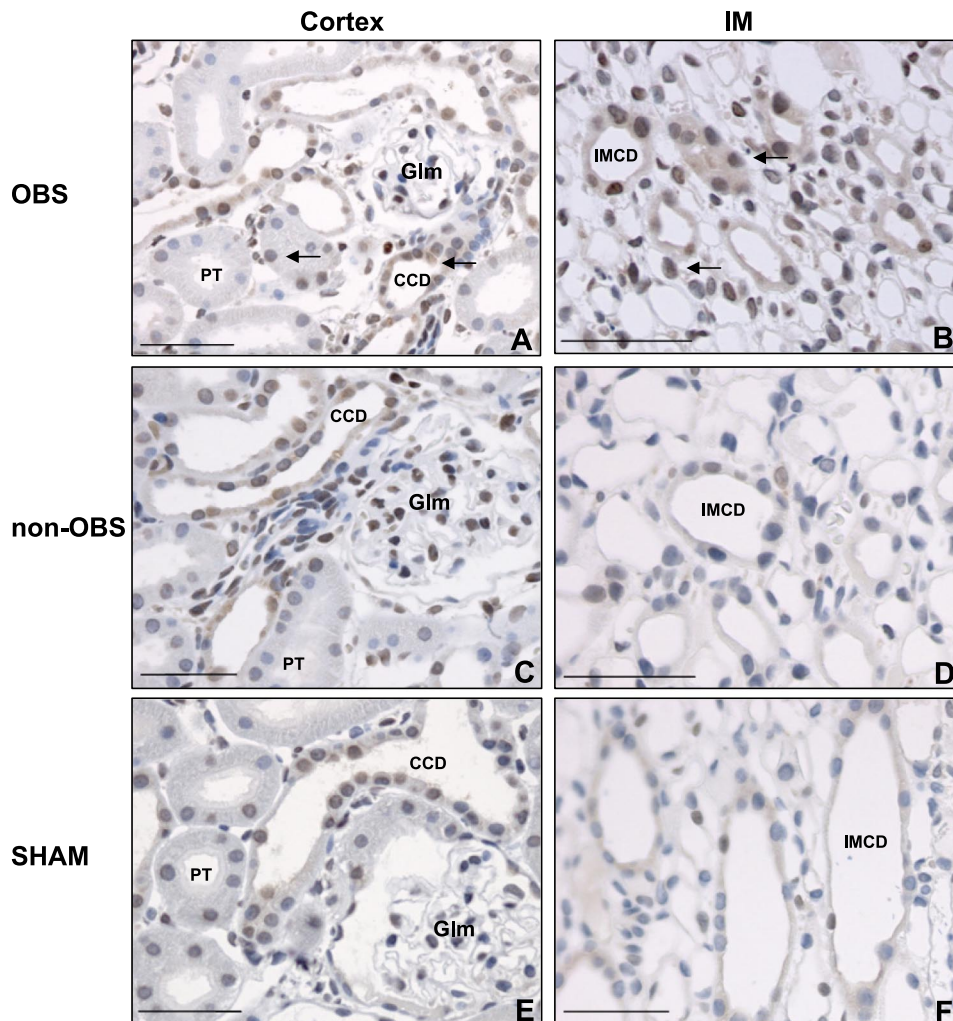
Fig. 5. Immunohistochemistry for AM in kidney cortex and IM from 24-h UUO rats (Obs and Non-obs) (*A–D*) and Sham rats (*E* and *F*). *A* and *B*: in the obstructed kidney of UUO rats, significant AM labeling was associated with PT, connecting tubuli, Glm, interstitial cells, and CCD (*A*) and IMCD, thin limbs of Henle's loop, papillary epithelium, and interstitial cells (*B*). *C* and *D*: in the nonobstructed kidney of UUO rats AM was comparable to that seen in obstructed kidneys in cortex (*C*). However, in IM from nonobstructed kidneys of UUO rats the AM labeling was comparable to that observed in sham-operated rats (*D*). *E* and *F*: in cortex from control kidneys, AM immunoreactivity was associated with connecting tubuli and cortical collecting ducts (*E*), and in the IM AM immunoreactivity was associated with IMCD and thin limbs of Henle's loop (*F*). Bar = 50 µm.

Increased TNF-α levels in inner medulla in response to 24-h BUO. TNF-α levels were measured in tissue homogenates from IM from both BUO and sham-operated control rats. Results showed that rats subjected to 24-h BUO had an increase in TNF-α concentration compared with Sham rats (1.08 ± 0.16 vs. 0.61 ± 0.07 pg/ml of protein; $P < 0.05$).

DISCUSSION

The main results of the present study were that AM mRNA, protein concentration, and tissue distribution increase in C+OM fraction and IM of kidneys in response to BUO. UUO was associated with a differential response: in IM, AM was increased only in the obstructed kidney whereas in C+OM fraction AM was increased both in obstructed and contralateral kidney compared with Sham. The tissue level of HIF-1α protein increased in the renal inner medulla of rats subjected to 24-h BUO. By immunohistochemical labeling, HIF-1α immunoreactive protein was virtually absent in control kidneys. In response to BUO, HIF-1α was associated predominantly with medullary collecting duct segments also positive for AM. The data show that BUO is associated with stimulation of HIF-1α in a pattern likely to reflect oxygen gradients and colocalization with AM in accordance with a role of HIF-1α for stimulation of AM. The present in vivo approach cannot establish whether

this relation is causal. The observation that HIF-1α and AM responded differentially in the C+OM tissue in response to obstruction suggests that hypoxia/HIF-1α is less likely to drive the observed increase in AM in C+OM. AM was elevated in C+OM in the contralateral, nonobstructed kidney in the UUO model, which is hyperperfused and not underperfused. Thus mechanisms not related to hypoxia/HIF-1α are likely to stimulate AM in C+OM.

AM is significantly regulated by tissue O_2 pressure. Hypoxic stimulation of AM has been reported in various cultured cells (38, 44) and in vivo in kidneys (13, 44), lungs (13), heart (13), and brain (13). In both normal and hypoxic kidneys there is an O_2 gradient with a progressive decrease toward the IM. This is due to the very low medullary perfusion coefficient, a high arteriovenous O_2 shunting in the cortical area, and a high O_2 extraction, which all converge to a very low partial O_2 pressure in IM (7). It is well known that ureteral obstruction is associated with a reduction in RBF (11, 16, 53), and since the IM receives less than 10% of total RBF (49) obstruction of the ureter leads to a very low partial O_2 pressure in IM. The marked stimulation of HIF-1α and AM in IM compared with cortex is consistent with the expected oxygen gradient. Immunohistochemical staining showed that HIF-1α was induced in both the nuclei and cytoplasma in collecting ducts, interstitial
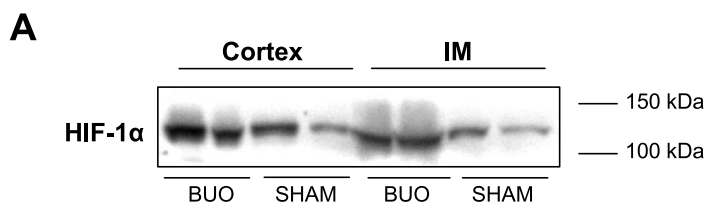
A

Fig. 6. Semiquantitative immunoblots of hypoxia inducible factor-1α (HIF-1α) using nuclear protein extract isolated from cortex and IM from 24-h BUO ($n = 6$) and Sham ($n = 6$) rats. A total of 50 μg protein was used for the HIF-1α assay. *A*: immunoblot was reacted with anti-HIF-1α antibody and revealed a single ~120-kDa band. Densitometric analyses of all the samples from sham-operated and obstructed kidneys of rats with 24-h BUO revealed that there was no difference between control and obstructed kidneys in cortex. However, HIF-1α protein expression was increased in IM in 24-h BUO compared with sham-operated rats. Immunohistochemistry for HIF-1α from kidney inner medulla IM of 24-h BUO (*B*) and sham-operated rats (*C*). *$P < 0.05$ BUO compared with sham rats. *B*: IM from obstructed kidneys, significant immunoreactivity for HIF-1α was associated with both nucleus and cytosol in IMCD, thin limbs of Henle's loop (TL) and interstitial cells. CD, Collecting duct. *C*: IM from control kidneys showed no HIF-1α immunoreactivity. Bar = 50 μm.
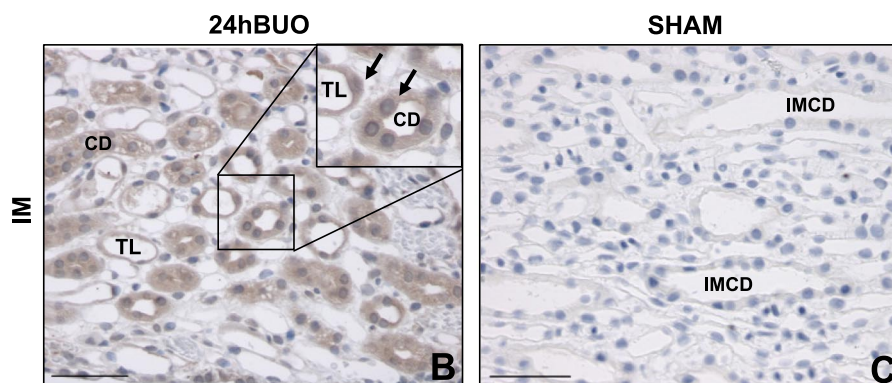
cells, and thin limbs of the loop of Henle of BUO kidneys. This is consistent with previous studies demonstrating inner medullary HIF-1α expression localized to the collecting ducts, interstitial cells, and thin limbs of the loop of Henle of hypoxic and ischemic kidneys (40). Previous findings have demonstrated that HIF-1α is primarily localized in the nuclei in response to hypoxia (40). However, we observe HIF-1α localization in both nuclei and cytoplasma in response to 24-h BUO. This staining pattern for HIF-1α was also observed in response to chemotherapy using amifostine (27), demonstrating an intense cytoplasmic and nuclear induction of HIF-1α in renal tubular epithelium after ligation of kidney vessels. The localization of AM and HIF-1α particularly in the collecting ducts

and thin limbs of the loop of Henle is compatible with the notion that AM transcription could be controlled by HIF-1α in response to 24-h BUO. AM is locally transcribed in these segments (45).

In addition to hypoxia, AM production is increased in conditions with inflammation, and it has been demonstrated that inflammatory cytokines, such as TNF-α and IL-1β stimulates AM (14, 31, 52, 55). Nitric oxide (NO) directly stimulates AM (14). Ureteral obstruction also leads to an intense infiltration of inflammatory cells (18, 32, 33). Consistent with previous studies demonstrating increased TNF-α expression, it is thus likely that inflammatory cytokines induced by the obstruction may be involved in the enhanced AM expression in
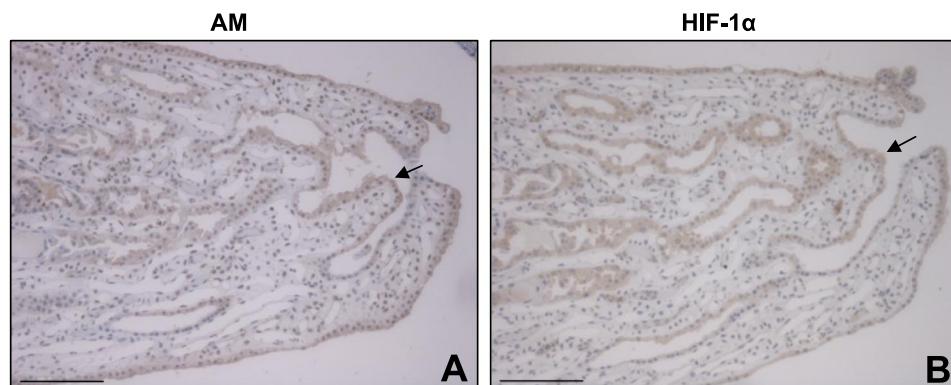

Fig. 7. Immunohistochemistry for AM (*A*) and HIF-1α (*B*) in 2 pairs of consecutive sections from IM from rats subjected to 24-h BUO. Sections were processed such that adjacent surfaces were stained. The almost complete overlap in expression of AM and HIF-1α in the tubular cells of the 2 sections should be noted. Bar = 200 μm.

response to urinary tract obstruction. Enhanced formation of NO by increased cortical blood flow with larger shear stress or by inflammatory cytokines could contribute to stimulation of AM independent of oxygen tension and HIF-1α.

After obstruction, AM immunoreactivity was most prominent in collecting ducts, interstitial cells, and thin limbs of the loop of Henle. These findings are consistent with findings by Hofbauer et al. (13), who showed localization of AM protein in the same segments. Furthermore, they also observed strong labeling of AM in both human and rat kidneys subjected to ischemia. AM mediates its effect by binding to its receptor, which comprises RAMPs and CRLR (23, 24). It has previously been demonstrated that RAMP1 and 3, as well as CRLR mRNA levels in whole kidney, is markedly upregulated in response to 6 and 14 days of UUO. However, these alterations appear to be ligand independent, since there was no significant change in the AM gene expression (37).

The present study demonstrated that AM mRNA and protein are increased in both C+OM and IM in the obstructed kidney compared with sham-operated rats in response to 24-h UUO. An interesting finding was that AM was enhanced equally in C+OM of obstructed and nonobstructed kidney in the UUO model. UUO decreases GFR and RBF in the obstructed kidney, and this is associated with compensatory increases in GFR and RBF in the nonobstructed contralateral kidney (10).

What is the physiological role of AM in obstructive nephropathy? A protective role for AM is likely to counter endothelial and renal tubular injury in an autocrine/paracrine manner (3, 25, 39). AM is a vasodilator and lowers renal vascular resistance (19). AM increases medullary blood flow and induces diuresis and natriuresis by inhibition of NaCl reabsorption (5, 22, 36). It is well accepted that GFR and RBF are consistently reduced after release of 24-h BUO (8, 10, 30). Furthermore, release of 24-h BUO is associated with a dramatically increased diuresis and natriuresis. It might therefore be speculated that upregulation of AM in response to urinary tract obstruction could contribute to preservation of medullary blood flow in the obstructed kidney. The increased levels of AM could facilitate the observed diuresis and natriuresis by inhibition of NaCl transport, which lowers oxygen demand (21, 22). Elucidation of these mechanisms awaits pharmacological tools to manipulate AM or kidney-specific deletion of the AM gene.

Perspectives and significance of the present findings. The present study using a targeted proteomics approach demonstrates that HIF-1α and the HIF target gene product AM exhibit significantly elevated levels in kidney IM after bilateral and unilateral ureteral obstruction in keeping with the anticipated oxygen gradients. The observation of increased levels of HIF-1α supports the notion that ureteral obstruction is associated with hypoxia, especially within the renal medulla. Further studies should clarify whether AM is important for prevention of tissue injury in response to urinary tract obstruction. Furthermore, it should also be elucidated whether AM expression is increased in the kidney in response to acute obstruction likely secondary to obstruction induced HIF-1α induction as a result of medullary hypoxia.

REFERENCES

1. **Cachat F, Lange-Sperandio B, Chang AY, Kiley SC, Thornhill BA, Forbes MS, Chevalier RL.** Ureteral obstruction in neonatal mice elicits segment-specific tubular cell responses leading to nephron loss. *Kidney Int* 63: 564–575, 2003.

2. **Cheung B, Leung R.** Elevated plasma levels of human adrenomedullin in cardiovascular, respiratory, hepatic and renal disorders. *Clin Sci (Lond)* 92: 59–62, 1997.

3. **Chini EN, Chini CC, Bolliger C, Jougasaki M, Grande JP, Burnett JC Jr, Dousa TP.** Cytoprotective effects of adrenomedullin in glomerular cell injury: central role of cAMP signaling pathway. *Kidney Int* 52: 917–925, 1997.

4. **Cormier-Regard S, Nguyen SV, Claycomb WC.** Adrenomedullin gene expression is developmentally regulated and induced by hypoxia in rat ventricular cardiac myocytes. *J Biol Chem* 273: 17787–17792, 1998.

5. **Ebara T, Miura K, Okumura M, Matsuura T, Kim S, Yukimura T, Iwao H.** Effect of adrenomedullin on renal hemodynamics and functions in dogs. *Eur J Pharmacol* 263: 69–73, 1994.

6. **Eickelberg O, Seebach F, Riordan M, Thulin G, Mann A, Reidy KH, Van Why SK, Kashgarian M, Siegel N.** Functional activation of heat shock factor and hypoxia-inducible factor in the kidney. *J Am Soc Nephrol* 13: 2094–2101, 2002.

7. **Epstein FH.** Oxygen and renal metabolism. *Kidney Int* 51: 381–385, 1997.

8. **Frokiaer J, Knudsen L, Nielsen AS, Pedersen EB, Djurhuus JC.** Enhanced intrarenal angiotensin II generation in response to obstruction of the pig ureter. *Am J Physiol Renal Fluid Electrolyte Physiol* 263: F527–F533, 1992.

9. **Ghafar MA, Anastasiadis AG, Olsson LE, Chichester P, Kaplan SA, Buttyan R, Levin RM.** Hypoxia and an angiogenic response in the partially obstructed rat bladder. *Lab Invest* 82: 903–909, 2002.

10. **Harris RH, Gill JM.** Changes in glomerular filtration rate during complete ureteral obstruction in rats. *Kidney Int* 19: 603–608, 1981.

11. **Hegarty NJ, Young LS, Kirwan CN, O'Neill AJ, Bouchier-Hayes DM, Sweeney P, Watson RW, Fitzpatrick JM.** Nitric oxide in unilateral ureteral obstruction: effect on regional renal blood flow. *Kidney Int* 59: 1059–1065, 2001.

12. **Hinson JP, Kapas S, Smith DM.** Adrenomedullin, a multifunctional regulatory peptide. *Endocr Rev* 21: 138–167, 2000.

13. **Hofbauer KH, Jensen BL, Kurtz A, Sandner P.** Tissue hypoxygenation activates the adrenomedullin system in vivo. *Am J Physiol Regul Integr Comp Physiol* 278: R513–R519, 2000.

14. **Hofbauer KH, Schoof E, Kurtz A, Sandner P.** Inflammatory cytokines stimulate adrenomedullin expression through nitric oxide-dependent and -independent pathways. *Hypertension* 39: 161–167, 2002.

15. **Hsu CH, Kurtz TW, Rosenzweig J, Weller JM.** Intrarenal hemodynamics and ureteral pressure during ureteral obstruction. *Invest Urol* 14: 442–445, 1977.

16. **Huland H, Leichtweiss HP, Schroder H, Jeschkies R.** Effects of ureteral obstruction on renal cortical blood flow. *Urol Int* 37: 213–219, 1982.

17. **Ishizaka Y, Ishizaka Y, Tanaka M, Kitamura K, Kangawa K, Minamino N, Matsuo H, Eto T.** Adrenomedullin stimulates cyclic AMP formation in rat vascular smooth muscle cells. *Biochem Biophys Res Commun* 200: 642–646, 1994.

18. **Ito K, Chen J, Vaughan ED Jr, Seshan SV, Poppas DP and Felsen D.** Dietary L-arginine supplementation improves the glomerular filtration rate and renal blood flow after 24 hours of unilateral ureteral obstruction in rats. *J Urol* 171: 926–930, 2004.

19. **Jensen BL, Kramer BK, Kurtz A.** Adrenomedullin stimulates renin release and renin mRNA in mouse juxtaglomerular granular cells. *Hypertension* 29: 1148–1155, 1997.

20. **Jiang BH, Rue E, Wang GL, Roe R, Semenza GL.** Dimerization, DNA binding, and transactivation properties of hypoxia-inducible factor 1. *J Biol Chem* 271: 17771–17778, 1996.

21. **Jougasaki M, Aarhus LL, Heublein DM, Sandberg SM, Burnett JC Jr.** Role of prostaglandins and renal nerves in the renal actions of adrenomedullin. *Am J Physiol Renal Physiol* 272: F260–F266, 1997.

22. **Jougasaki M, Wei CM, Aarhus LL, Heublein DM, Sandberg SM, Burnett JC Jr.** Renal localization and actions of adrenomedullin: a natriuretic peptide. *Am J Physiol Renal Fluid Electrolyte Physiol* 268: F657–F663, 1995.

23. **Kamitani S, Asakawa M, Shimekake Y, Kuwasako K, Nakahara K, Sakata T.** The RAMP2/CRLR complex is a functional adrenomedullin receptor in human endothelial and vascular smooth muscle cells. *FEBS Lett* 448: 111–114, 1999.

24. **Kapas S, Catt KJ, Clark AJ.** Cloning and expression of cDNA encoding a rat adrenomedullin receptor. *J Biol Chem* 270: 25344–25347, 1995.

25. **Kato H, Shichiri M, Marumo F, Hirata Y.** Adrenomedullin as an autocrine/paracrine apoptosis survival factor for rat endothelial cells. *Endocrinology* 138: 2615–2620, 1997.

26. **Kitamura K, Kangawa K, Kawamoto M, Ichiki Y, Nakamura S, Matsuo H, Eto T.** Adrenomedullin: a novel hypotensive peptide isolated from human pheochromocytoma. *Biochem Biophys Res Commun* 192: 553–560, 1993.

27. **Koukourakis MI, Giatromanolaki A, Chong W, Simopoulos C, Polychronidis A, Sivridis E, Harris AL.** Amifostine induces anaerobic metabolism and hypoxia-inducible factor 1 alpha. *Cancer Chemother Pharmacol* 53: 8–14, 2004.

28. **Kureishi Y, Kobayashi S, Nishimura J, Nakano T, Kanaide H.** Adrenomedullin decreases both cytosolic Ca^{2+} concentration and Ca^{2+}-sensitivity in pig coronary arterial smooth muscle. *Biochem Biophys Res Commun* 212: 572–579, 1995.

29. **Leonard MO, Cottell DC, Godson C, Brady HR, Taylor CT.** The role of HIF-1 alpha in transcriptional regulation of the proximal tubular epithelial cell response to hypoxia. *J Biol Chem* 278: 40296–40304, 2003.

30. **Li C, Wang W, Kwon TH, Isikay L, Wen JG, Marples D, Djurhuus JC, Stockwell A, Knepper MA, Nielsen S, Frokiær J.** Downregulation of AQP1, -2, and -3 after ureteral obstruction is associated with a long-term urine-concentrating defect. *Am J Physiol Renal Physiol* 281: F163–F171, 2001.

31. **Li YY, Wong LY, Cheung BM, Hwang IS, Tang F.** Differential induction of adrenomedullin, interleukins and tumour necrosis factor-alpha by lipopolysaccharide in rat tissues in vivo. *Clin Exp Pharmacol Physiol* 32: 1110–1118, 2005.

32. **Meldrum KK, Metcalfe P, Leslie JA, Misseri R, Hile KL, Meldrum DR.** TNF-alpha neutralization decreases nuclear factor-kappaB activation and apoptosis during renal obstruction. *J Surg Res* 131: 182–188, 2006.

33. **Misseri R, Meldrum DR, Dagher P, Hile K, Rink RC, Meldrum KK.** Unilateral ureteral obstruction induces renal tubular cell production of tumor necrosis factor-alpha independent of inflammatory cell infiltration. *J Urol* 172: 1595–1599, 2004.

34. **Moody TE, Vaughan ED Jr, Gillenwater JY.** Comparison of the renal hemodynamic response to unilateral and bilateral ureteral occlusion. *Invest Urol* 14: 455–459, 1977.

35. **Moody TE, Vaughn ED Jr, Gillenwater JY.** Relationship between renal blood flow and ureteral pressure during 18 hours of total unilateral urethetral occlusion Implications for changing sites of increased renal resistance. *Invest Urol* 13: 246–251, 1975.

36. **Mori Y, Nishikimi T, Kobayashi N, Ono H, Kangawa K, Matsuoka H.** Long-term adrenomedullin infusion improves survival in malignant hypertensive rats. *Hypertension* 40: 107–113, 2002.

37. **Nagae T, Mukoyama M, Sugawara A, Mori K, Yahata K, Kasahara M, Suganami T, Makino H, Fujinaga Y, Yoshioka T, Tanaka I, Nakao K.** Rat receptor-activity-modifying proteins (RAMPs) for adrenomedullin/CGRP receptor: cloning and upregulation in obstructive nephropathy. *Biochem Biophys Res Commun* 270: 89–93, 2000.

38. **Nguyen SV, Claycomb WC.** Hypoxia regulates the expression of the adrenomedullin and HIF-1 genes in cultured HL-1 cardiomyocytes. *Biochem Biophys Res Commun* 265: 382–386, 1999.

39. **Nishimatsu H, Hirata Y, Shindo T, Kurihara H, Kakoki M, Nagata D, Hayakawa H, Satonaka H, Sata M, Tojo A, Suzuki E, Kangawa K, Matsuo H, Kitamura T, Nagai R.** Role of endogenous adrenomedullin in the regulation of vascular tone and ischemic renal injury: studies on transgenic/knockout mice of adrenomedullin gene. *Circ Res* 90: 657–663, 2002.

40. **Rosenberger C, Mandriota S, Jurgensen JS, Wiesener MS, Horstrup JH, Frei U, Ratcliffe PJ, Maxwell PH, Bachmann S, Eckardt KU.** Expression of hypoxia-inducible factor-1alpha and -2alpha in hypoxic and ischemic rat kidneys. *J Am Soc Nephrol* 13: 1721–1732, 2002.

41. **Ruiz-Deya G, Sikka SC, Thomas R, Abdel-Mageed AB.** Potential role for the nuclear transcription factor NF-kappa B in the pathogenesis of ureteropelvic junction obstruction. *J Endourol* 16: 611–615, 2002.

42. **Sakata J, Shimokubo T, Kitamura K, Nakamura S, Kangawa K, Matsuo H, Eto T.** Molecular cloning and biological activities of rat adrenomedullin, a hypotensive peptide. *Biochem Biophys Res Commun* 195: 921–927, 1993.

43. **Sakata J, Shimokubo T, Kitamura K, Nishizono M, Iehiki Y, Kangawa K, Matsuo H, Eto T.** Distribution and characterization of immunoreactive rat adrenomedullin in tissue and plasma. *FEBS Lett* 352: 105–108, 1994.

44. **Sandner P, Hofbauer KH, Tinel H, Kurtz A, Thiesson HC, Ottosen PD, Walter S, Skott O, Jensen BL.** Expression of adrenomedullin in hypoxic and ischemic rat kidneys and human kidneys with arterial stenosis. *Am J Physiol Regul Integr Comp Physiol* 286: R942–R951, 2004.

45. **Semenza GL.** HIF-1: mediator of physiological and pathophysiological responses to hypoxia. *J Appl Physiol* 88: 1474–1480, 2000.

46. **Shimekake Y, Nagata K, Ohta S, Kambayashi Y, Teraoka H, Kitamura K, Eto T, Kangawa K, Matsuo H.** Adrenomedullin stimulates two signal transduction pathways, cAMP accumulation and Ca^{2+} mobilization, in bovine aortic endothelial cells. *J Biol Chem* 270: 4412–4417, 1995.

47. **Siegel NJ, Feldman RA, Lytton B, Hayslett JP, Kashgarian M.** Renal cortical blood flow distribution in obstructive nephropathy in rats. *Circ Res* 40: 379–384, 1977.

48. **Sugo S, Minamino N, Shoji H, Kangawa K, Kitamura K, Eto T, Matsuo H.** Production and secretion of adrenomedullin from vascular smooth muscle cells: augmented production by tumor necrosis factor-alpha. *Biochem Biophys Res Commun* 203: 719–726, 1994.

49. **Sweeney P, Young LS, Fitzpatrick JM.** An autoradiographic study of regional blood flow distribution in the rat kidney during ureteric obstruction—the role of vasoactive compounds. *BJU Int* 88: 268–272, 2001.

50. **Vaughan ED Jr, Shenasky JH, Gillenwater JY.** Mechanism of acute hemodynamic response to ureteral occlusion. *Invest Urol* 9: 109–118, 1971.

51. **Wiener CM, Booth G, Semenza GL.** In vivo expression of mRNAs encoding hypoxia-inducible factor 1. *Biochem Biophys Res Commun* 225: 485–488, 1996.

52. **Wong LY, Cheung BM, Li YY, Tang F.** Adrenomedullin is both proinflammatory and antiinflammatory: its effects on gene expression and secretion of cytokines and macrophage migration inhibitory factor in NR8383 macrophage cell line. *Endocrinology* 146: 1321–1327, 2005.

53. **Yarger WE, Griffith LD.** Intrarenal hemodynamics following chronic unilateral ureteral obstruction in the dog. *Am J Physiol* 227: 816–826, 1974.

54. **Yarger WE, Schocken DD, Harris RH.** Obstructive nephropathy in the rat: possible roles for the renin-angiotensin system, prostaglandins, and thromboxanes in postobstructive renal function. *J Clin Invest* 65: 400–412, 1980.

55. **Zhou M, Chaudry IH, Wang P.** Adrenomedullin is upregulated in the heart and aorta during the early and late stages of sepsis. *Biochim Biophys Acta* 1453: 273–283, 1999.